Novel Magnetism in ^{3}He Nanoclusters

N. Matsunaga,[1,*] V. A. Shvarts,[2] E. D. Adams,[1,†] J. S. Xia,[2] and E. A. Schuberth[3]

[1]*Center for Ultralow Temperature Research, Department of Physics, University of Florida, Gainesville, Florida 32611-8440*

[2]*NMHFL, Department of Physics, University of Florida, Gainesville, Florida 32611-8440*

[3]*Walther-Meissner Institut, D-85748 Garching, Germany*

(Received 28 September 2000)

The magnetic susceptibility of ^{3}He nanoclusters embedded in a ^{4}He matrix has been measured from 0.5 to 10 mK at pressures from 2.88 to 3.54 MPa. Even the lowest pressure clusters have a solid fraction in the region of the phase diagram where bulk solid is unstable. At 3.54 MPa, $\theta = -250$ μK, equal to that of bulk ^{3}He for $v = 21.3$ cm^3/mole. For 2.88 MPa, $\theta = 140$ μK, indicating a ferromagnetic tendency, similar to 2D films at some coverages. At intermediate pressures, χ has a peak near 1.05 mK, but with no discontinuity. Magnetic ordering in nanoclusters appears to be different than the U2D2 phase of bulk ^{3}He.

DOI: 10.1103/PhysRevLett.86.2365 PACS numbers: 67.80.Gb, 67.80.Jd, 75.30.Kz, 75.60.Nt

Recent studies of solid and liquid clusters and films have shown that their properties are quite different from those of bulk condensed matter [1–3]. Pure bulk ^{3}He at melting pressure orders antiferromagnetically at $T_N = 0.9$ mK in a U2D2 magnetic structure in low magnetic fields [4]. A second ordered phase, thought to be a canted antiferromagnet, occurs above 0.45 T [5,6]. In films of ^{3}He on a Grafoil substrate, direct particle exchange is responsible for exotic phases in which a competition between multiparticle exchange processes leads to frustration [1,2]. Nanoclusters of ^{3}He, the size and state of which depend on the initial ^{3}He concentration and external pressure, can be produced by isotopic phase separation of ^{3}He-^{4}He mixtures. For concentrations $\sim$1%, all solid, partially liquid, or totally liquid nanoclusters with size distribution averaging $\sim$20 nm are produced at various growth pressures in 100 nm pore in metal sinters [3]. The magnetic properties of nanoclusters and how they compare with bulk ^{3}He are of considerable interest.

Previously, Schrenk *et al.* [3] have observed a history-dependent maximum in the heat capacity of clusters embedded in a ^{4}He matrix at $T \sim 1$ mK, for pressures as low as 2.80 MPa. They interpreted the maximum as the Néel temperature T_N in the clusters, which, when plotted versus pressure, suggested a smooth continuation of $T_N(P)$ of pure bulk ^{3}He. However, they did not see the latent-heat peak characteristic of the first-order transition in pure bulk ^{3}He [7] and integration of C/T through the peak indicates that much of the spin entropy, $S = R \ln 2$, remained at their lowest temperature [8].

We have studied the magnetic susceptibility of ^{3}He nanoclusters from 0.5 to 10 mK at pressures from 2.88 to 3.54 MPa. We find that even the lowest-pressure clusters have a solid fraction in the region of the phase diagram where bulk solid is unstable. The magnetization of the 3.54 MPa sample behaves similarly to that of bulk ^{3}He for $v = 21.3$ cm^3/mole, with a Weiss constant $\theta = -250$ μK. For 2.88 MPa for which the solid fraction is only 0.19, χ follows a Curie-Weiss law with a *positive* $\theta = 140$ μK, indicative of a ferromagnetic tendency, similar to that seen in 2D films at some coverages. At intermediate pressures, we find a peak in χ, indicative of ordering, near 1.05 mK, but with no discontinuity. Magnetic ordering in ^{3}He nanoclusters appears to be quite different than for bulk ^{3}He, not an extension of the U2D2 phase to lower pressures.

As shown in the inset of Fig. 1, the experimental cell is made of a Vespel cylinder 3 mm in diameter $\times$ 10 mm long. The heat exchanger was made of 70 nm silver powder packed at 20 MPa around a 0.5-mm diam silver wire welded to the silver support. A miniature coin-silver pressure transducer was glued to the end of the Vespel tube.

Separate NMR transmitter and receiver coils were supported from the $PrNi_5$ cooling stage to avoid heating of the sample by the pulses. A PLM-4 pulsed NMR spectrometer [9] operating at 125 or 250 kHz was used for measuring the susceptibility and spin-lattice relaxation times, T_1. Magnetization measurements were spaced several times T_1, which at the lowest temperature required 6–8 hours between points. The free induction decay was recorded in a digital oscilloscope, then read into a computer for performing the Fourier transform (FT), with a frequency resolution of 10 Hz. The magnetic susceptibility was obtained by integrating the FT over a frequency range of 20 kHz.

Temperatures were produced by a $PrNi_5$ demagnetization stage and were measured with a ^{3}He melting pressure thermometer [10]. Samples were formed by the blocked capillary technique and annealed 1–4 days at temperatures near 1.7–1.9 K to minimize pressure gradients. Then, samples were slowly cooled through the phase-separation temperature, $T_{ps} \approx 170$ mK, which was observed by the pressure change.

Shown in Fig. 1 are the P-T phase diagrams of pure ^{3}He and ^{4}He and of mixtures [11] of the two, along with the pressures of the samples for our ^{3}He concentration $x = 0.006$ (shown only as horizontal lines). In mixtures following phase separation, melting in one of the phases occurs along the univariant (three phases in equilibrium), shown

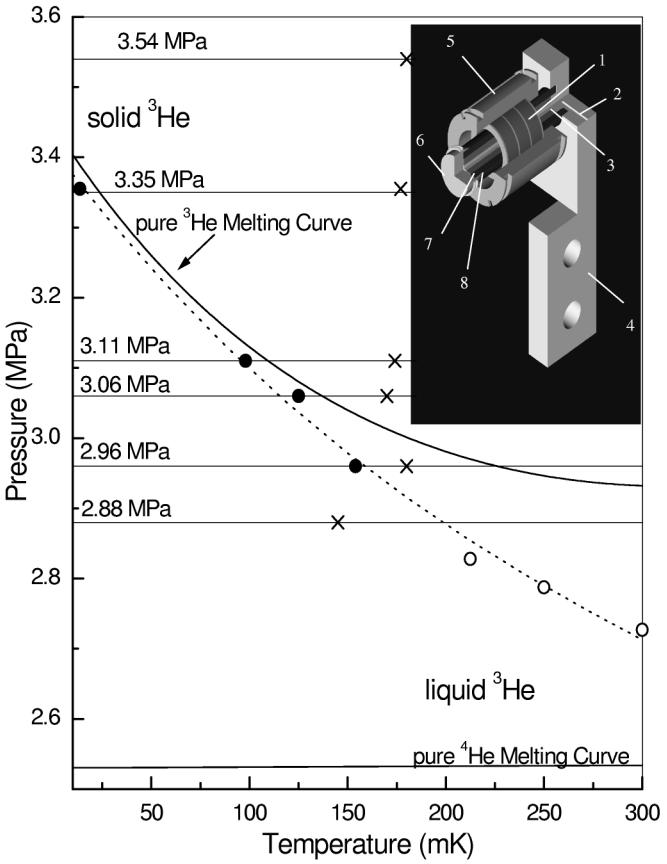

FIG. 1. Sample pressures studied with the P-T phase diagrams of pure ^{3}He, ^{4}He , and mixtures. Open circles are from Ref. [11], closed circles are our univariant points, and crosses are phase-separation temperatures. The dotted line is a fit to the univariant. The inset shows the experimental cell setup. 1: Excitation and pickup coil; 2: mixture fill line; 3: silver wire; 4: silver thermal link; 5: excitation coil (not used); 6: coin-silver pressure transducer; 7: silver powder; 8: Vespel-22 sample cell.

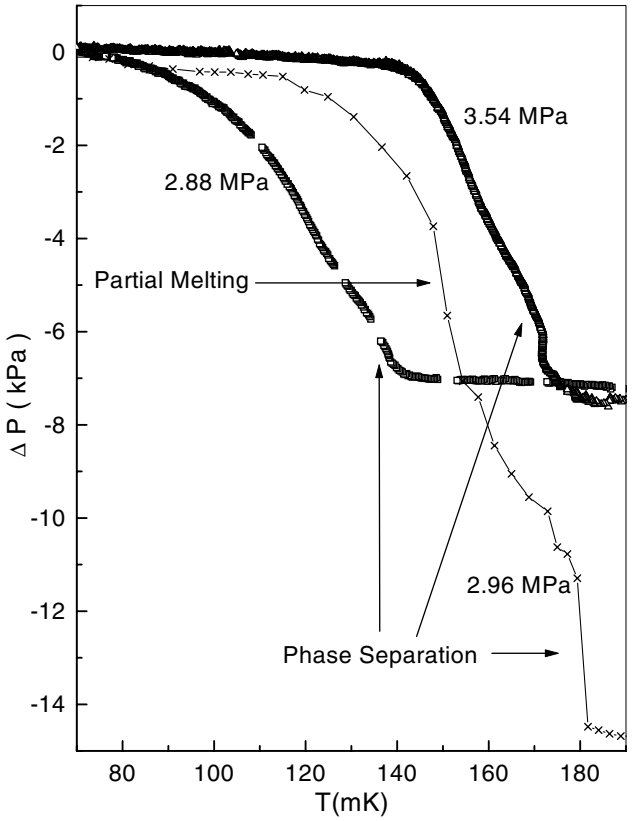

FIG. 2. Pressure changes relative to $P(T = 0)$ for the three samples, showing phase separation and partial melting.

by the circles and dashed line [11]. Pressure changes on phase separation and melting are shown in Fig. 2 for three representative pressures.

Based on equilibrium thermodynamics for bulk quantities of ^{3}He and ^{4}He, phase-separated mixtures would be expected to melt *completely* as they are cooled along the univariant line, with solid being unstable in the two-phase region below the univariant. However, from the change in pressure across the univariant and the susceptibility, as discussed below, we see that the clusters melt only *partially*. Some solid ^{3}He remains in the two-phase region where only liquid ^{3}He and solid ^{4}He would be expected. We find a solid fraction even at 2.88 MPa, well below the univariant, where bulk solid ^{3}He is unstable. Clearly, the nanoclusters do not behave like bulk ^{3}He. As presented below, their magnetic properties are quite different from those of bulk solid ^{3}He.

The susceptibility is a sum of solid and liquid contributions, χ_{solid} and χ_{liquid}, respectively. In the "high-T" region above about 2 mK, the solid susceptibility, to a good approximation, follows the Curie-Weiss law, $\chi_{\text{solid}} \approx C_s/(T - \theta)$, where θ is the Weiss temperature and C_s is $\sim N_{\text{solid}}$, the number of nuclei in the solid phase. The liquid has the temperature-independent Fermi-liquid behavior, $\chi_{\text{liquid}} = 3C_l/2T_F^{**}$, where C_l is the Curie constant $\sim N_{\text{liquid}}$, the number of ^{3}He nuclei in the liquid phase, and T_F^{**} is the effective Fermi temperature $\sim$280–300 mK. For equal quantities of solid and liquid, the ratio of signals at 10 mK is $\chi_{\text{solid}}/\chi_{\text{liquid}} \cong 20$, increasing to $\cong$100 at 2 mK. Thus, in our measurements, χ_{liquid} is a constant $\ll \chi_{\text{solid}}$ which we include in the subtraction of the background signal (spectrometer reading with no ^{3}He signal). Then, the temperature-dependent remaining signal gives an accurate determination of the solid fraction of the clusters.

For samples at $P < 3.54$ MPa that undergo partial melting upon cooling below the univariant, the fraction of solid in the clusters is given by $\chi_{\text{solid}}(P)/\chi_{\text{solid}}(3.54)$ since there is no liquid present at the higher pressure. (We neglect a small compressibility correction $\sim$1–2%.) The solid fraction increases from 0.2 to 1.0 as the pressure is increased from 2.88 to 3.54 MPa, and exists in the region of the P-T phase diagram where pure bulk solid ^{3}He is unstable. The likely explanation is that the van der Waals attraction of the denser ^{4}He matrix produces a few dense surface layers of solid ^{3}He at the cluster interface. For our lowest

pressure (see below), only two or three layers are required to account for the solid fraction. Hata *et al.* [12] found a surface magnetization of pure ^{3}He on silver corresponding to about ten layers at 2.9 MPa.

The temperature dependence of the susceptibility for the all-solid 3.54 MPa sample (see Figs. 1 and 2) is shown in Fig. 3 as χ^{-1} versus T in which θ is the intercept on the T axis. We find two different linear regions for high T and low T, as shown by the dashed and solid lines, similar to that seen in pure bulk solid ^{3}He [12]. (If all the data are fitted to a single straight line, the fit is significantly poorer.) The fit to the Curie-Weiss law above 4 mK gives $\theta \cong -250\ \mu$K. Using the same scaling law $\theta(v)$ found by Hata *et al.,* our θ corresponds to $v_{\text{bulk}} = 21.3\ \text{cm}^3/\text{mole}$, which is significantly less than v_{bulk} ($P = 3.54$). This is further indication that the van der Waals interaction with the dense hcp ^{4}He matrix ($v = 20.95\ \text{cm}^3/\text{mole}$) strongly affects the ^{3}He in the cluster. We find no ordering down to 0.55 mK at 3.54 MPa, whereas bulk ^{3}He at this pressure orders at $T_N \cong -\theta/2 = 0.9$ mK [12].

The susceptibilities of three samples at 2.96, 3.06, and 3.11 MPa, which have solid fractions of 0.23, 0.54, and 0.56, respectively, all behaved similarly. Data for the 2.96 MPa sample at 125 and 250 kHz are shown in Fig. 4 as M vs T^{-1}, which displays the low temperature behavior effectively. These data have been scaled in the high-T region so that $M(250) = 2M(125)$. The most interesting feature is the peak in M at $T \approx 1.09$ mK, which indicates the onset of ordering. The behavior at 125 kHz below the peak is similar to that of the U2D2 phase of bulk ^{3}He [12] where there is a discontinuous drop in M to 0.4 of its value at T_N. Our data do not show the discontinuity of the U2D2 phase; however, this could be rounding caused by size effects. For 250 kHz ($B = 0.078$ T), M is essentially constant from 1 to 0.8 mK, where it then begins to increase slightly upon further cooling. This is inconsistent with the U2D2 phase for which M is independent of field up to the critical field $B_{\text{cl}} = 0.4$ T. Thus, ordering in nanoclusters seen at these pressures is different than in bulk ^{3}He.

All three of the samples at pressures of 2.96, 3.06, and 3.11 MPa showed behavior similar to that described for 2.96 MPa. The temperatures of the peaks in χ are somewhat lower than the extension of $T_N(P)$ for the bulk and the pressure dependence is weaker. Our peak in χ is near the lowest "history-dependent" peak in the heat capacity seen by Schrenk *et al.* at the same pressures [3]. We looked for history dependence in χ by cooling to several different minimum temperatures before subsequently warming for a sample at 2.96 MPa (not shown). Although there was a slight difference in χ on warming and cooling, contrary to Schrenk *et al.* [3], we found no discernible difference in the temperature of the peak for different minimum temperatures.

We found a shift in the NMR frequency of only +20 Hz on cooling from the peak in χ to 0.5 mK. Also we found no resonances away from the Larmor frequency upon slowly ramping down the NMR field over a period of 96 h while applying pulses every 2 h. In the clusters, there are possibly many small domains at random orientations, which could spread out the resonance spectrum [4]. Also, we observed no changes in the fast, Zeeman exchange, part of T_1 and the spin-spin relaxation time T_2, which is sensitive to interactions between spins.

As shown in Figs. 1 and 2, the lowest pressure sample at 2.88 MPa phase separated at 145 mK, lower than 170–180 mK for all the others. At this pressure and

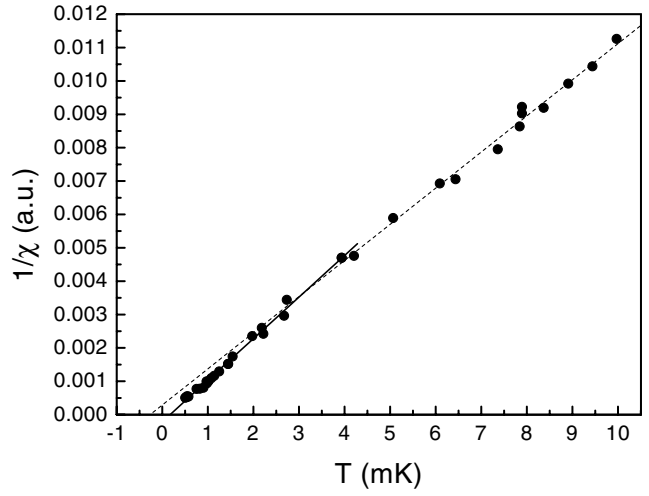

FIG. 3. Inverse of χ versus T for the 3.54 MPa sample.

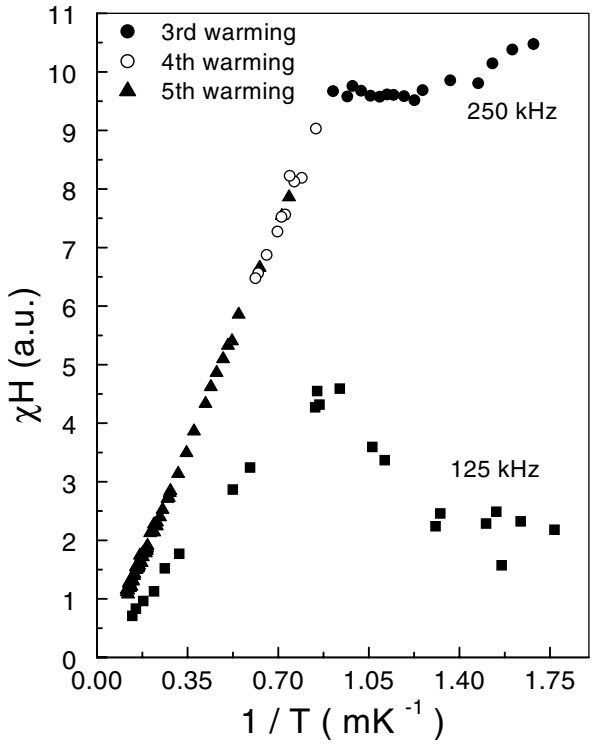

FIG. 4. Magnetization versus T^{-1} for the 3.06 MPa sample.

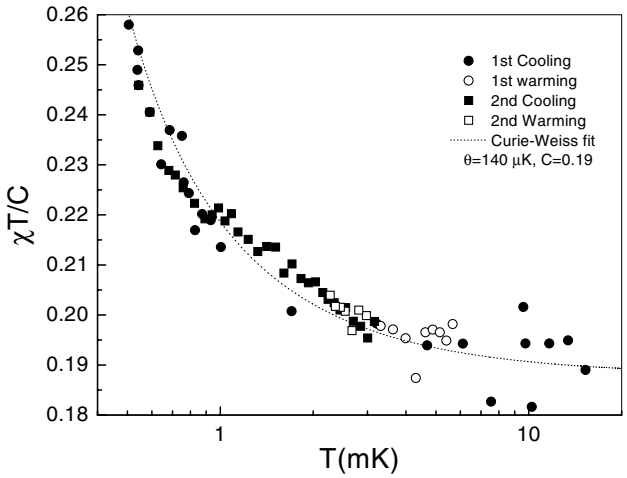

FIG. 5. Magnetic susceptibility times T/C versus T for the 2.88 MPa sample.

temperature, the ^{3}He enriched phase should precipitate as a liquid since it is in the two-phase region below the univariant. Thus, the pressure increase should include both the excess pressure of phase separation and the increase upon melting. However, the pressure increase shown in Fig. 2 is less than that for phase separation plus partial melting of the other samples. We attribute this to the fact that the matrix was in the bcc region of the phase diagram at the annealing temperature of this sample, and no evidence of the bcc-hcp crystallographic transition was seen on cooling. Thus it appears that in this case the ^{4}He remained in a metastable bcc state, rather than hcp.

The susceptibility for the sample at 2.88 MPa is shown in Fig. 5 as $\chi T/C$ versus T (semilog plot), which effectively displays the low-T region and departures from the Curie law. The dotted line is a fit to the Curie-Weiss law with $C/C(3.54) = 0.19$ (the fraction of solid in the cluster) and $\theta = +140\ \mu$K. The positive value of θ determined by the upward curvature indicates a *ferromagnetic* tendency. In the multiple-exchange model, exchanges of an odd number of particles, e.g., three, would lead to ferromagnetic interactions. Depending on the relative strengths of various exchange frequencies, a ferromagnetic transition would be expected at $T_C \approx \theta/2 = 70\ \mu$K [13,14].

The solid fraction of 0.19 for this sample would occupy only two or three layers on the bcc ^{4}He surface surrounding the cluster, possibly grown epitaxially. Our results for the 2.88 MPa sample may be compared with those for 2D ^{3}He films on Grafoil [1], for which both ferromagnetic and antiferromagnetic behaviors have been observed. For two different coverages showing ferromagnetic behavior, fits to the Curie-Weiss law gave θ's of 100 and 180 μK [2], compared with our value of 140 μK.

In summary, we find the magnetic properties of nanoclusters to be quite different from those of bulk ^{3}He. We find no ordering for all-solid clusters nor for the lowest pressure where the solid fraction is ≤ 0.2. At intermediate pressures for clusters that undergo partial melting, a peak in χ is observed near 1.0 mK. However, the 60% drop in χ at T_N seen in bulk solid ^{3}He does not occur in the nanoclusters. The susceptibility shows a solid fraction in the nanoclusters in the two-phase region of the phase diagram where bulk solid ^{3}He is unstable. Our measurements fail to support the conclusions of Schrenk *et al.* that ^{3}He nanoclusters undergo magnetic ordering at T_N (P) that is an extension of T_N of the bulk solid. A possible explanation for the history dependence seen in the heat capacity measurements of Schrenk *et al.* could be the short time scale for those measurements compared with the 6–8 hours for equilibrium between the clusters and the thermometer that we find.

This work has been supported by the National Science Foundation through Grants No. DMR-942103 and No. DMR-9800712. We thank Kevin Kless for help in preparing the manuscript for electronic submission. One of us (E. A. S.) thanks DAAD for support while at the University of Florida.

*Present address: NEC Corporation, 1120 Shimokuzawa, Sagamihara, Kanagawa Prefecture, Japan.
†Corresponding author.
Email address: adams@phys.ufl.edu

[1] M. Roger, C. Bäerle, Yu. M. Bunkov, A.-S. Chen, and H. Godfrin, Phys. Rev. Lett. **80**, 1308 (1998); C. Bäerle, J. Bossy, Yu. M. Bunkov, A.-S. Chen, H. Godfrin, and M. Roger, J. Low Temp. Phys. **110**, 345 (1998). See additional papers on 2D films in J. Low Temp. Phys. **110**.
[2] H. Ikegami, K. Obara, D. Ito, and H. Ishimoto, J. Low Temp. Phys. **113**, 277 (1998).
[3] R. Schrenk, R. König, and F. Pobell, Phys. Rev. Lett. **76**, 2945 (1996).
[4] D. D. Osheroff, M. C. Cross, and D. S. Fisher, Phys. Rev. Lett. **44**, 792 (1980).
[5] M. Roger, J. H. Hetherington, and J. M. Delrieux, Rev. Mod. Phys. **55**, 1 (1983).
[6] J. S. Xia, W. Ni, and E. D. Adams, Phys. Rev. Lett. **70**, 1481 (1993).
[7] D. S. Greywall and P. A. Busch, Phys. Rev. B **36**, 6853 (1987).
[8] E. D. Adams, R. P. Haley, and W. Ni, Phys. Rev. Lett. **77**, 5308 (1996).
[9] PLM-4, RV-Elektroniikka Oy Picowatt, SF-01510 Vantaa, Finland.
[10] W. Ni, J. S. Xia, E. D. Adams, P. S. Haskins, and J. E. McKisson, J. Low Temp. Phys. **99**, 167 (1995).
[11] P. M. Tedrow and D. M. Lee, Phys. Rev. **181**, 399 (1969).
[12] T. Hata, S. Yamasaki, T. Kodama, and T. Shigi, J. Low Temp. Phys. **71**, 193 (1988).
[13] H. Yano, H. Kondo, T. Suzuki, Y. Minamide, T. Kato, Y. Miura, and T. Mamiya, Phys. Rev. Lett. **65**, 3401 (1990).
[14] M. Roger, E. Suaudeau, and M. E. R. Bernier, Phys. Rev. B **35**, 2091 (1987).